http://dx.doi.org/10.5012/bkcs.2014.35.7.2013

DFT Study for Adsorption and Decomposition Mechanism of Trimethylene Oxide on Al(111) Surface

Cai-Chao Ye, Jie Sun,[†] Feng-Qi Zhao,[‡] Si-Yu Xu,[‡] and Xue-Hai Ju[*]

Key Laboratory of Soft Chemistry and Functional Materials of MOE, School of Chemical Engineering, Nanjing University of Science and Technology, Nanjing 210094, P.R. China. [*]E-mail: xhju@mail.njust.edu.cn
[†]State Key Laboratory of Natural Medicines, Jiangsu Key Laboratory of Carcinogenesis and Intervention, China Pharmaceutical University, Nanjing 210009, P.R. China
[‡]Science and Technology on Combustion and Explosion Laboratory, Xi'an Modern Chemistry Research Institute, Xi'an 710065, P.R. China
Received January 26, 2014, Accepted March 11, 2014

The adsorption and decomposition of trimethylene oxide (C_3H_6O) molecule on the Al(111) surface were investigated by the generalized gradient approximation (GGA) of density functional theory (DFT). The calculations employed a supercell ($6 \times 6 \times 3$) slab model and three-dimensional periodic boundary conditions. The strong attractive forces between C_3H_6O molecule and Al atoms induce the C-O bond breaking of the ring C_3H_6O molecule. Subsequently, the dissociated radical fragments of C_2H_6O molecule oxidize the Al surface. The largest adsorption energy is about −260.0 kJ/mol in **V3**, **V4** and **P2**, resulting a ring break at the C-O bond. We also investigated the decomposition mechanism of C_3H_6O molecules on the Al(111) surface. The activation energies (E_a) for the dissociations **V3**, **V4** and **P2** are 133.3, 166.8 and 174.0 kJ/mol, respectively. The hcp site is the most reactive position for C_3H_6O decomposing.

Key Words : Trimethylene oxide, Adsorption and dissociation, Al(111) surface, Density functional theory

Introduction

The composite mixtures of high performance energetic materials (EMs), with powderized aluminum (Al) and energetic binders as additives, are the most frequently used formulations in solid rocket propellant.[1] Nowadays, the using of active metallic additive to improve the performance of energetic materials becomes more and more important and popular in rocket propellant formulations. Researchers have studied reaction between explosives and Al surface, in order to understand the interaction mechanisms.[2,3] For example, Bucher *et al.* found that the combustion products such as Al_2O_3 are accompanied by a large amount of heat release, which could do benefit to increasing the combustion exothermicity.[4] Umezawa *et al.* investigated the decomposition and chemisorption of RDX (hexahydro-1,3,5-trinitro-1,3,5-triazine) molecule on Al(111) surface using molecular dynamics simulations.[5] Balbuena employed DFT method to characterize the infrared and terahertz spectra of a RDX deposited over an aluminum surface, which was modeled as a planar cluster of Al_{16}.[6] Sorescu *et al.* used first-principles method to calculated the adsorption of FOX-7 (1,1-Diamino-2,2-dinitroethylene) molecules on the α-Al_2O_3(0001) surface.[7,8] They also studied five adsorption configurations of FOX-7 on Al(111) surface, and discussed the geometries and energies.[9] In conclusion, as additives, Al powder is known to increase the combustion exothermicity and regression rate of solid propellant grains and enhance the blast effect of explosives as well as their underwater performance.[10] The efficiency of such processes depends on the size of the Al particles. Because the reducing the size of Al particles can accelerate burn rates of Al powders, Al nanopowder can significantly improve the performance of some energetic materials. Recently, our group also has studied the interaction mechanisms of nitroamine, FOX-7 and RDX molecules with Al powders by DFT method.[11-14] However, as an essential component of solid propellant, nowadays the studies about the interaction between binders with other ingredients (such as Al powder) in solid propellants are not available. Trimethylene oxide, also named oxetane (C_3H_6O), is a popular energetic binder for solid propellants and has been used to improve the low vulnerability of mixed explosives and solid propellant. While there are many reports about the reaction characteristics of Al surface with EMs, What is the adsorption and decomposition mechanism for trimethylene oxide on Al surface? So it seems interesting and necessary to understand the interaction between binders (trimethylene oxide) with Al powders.

Our work focuses on the detailed atomic-level description of the interactions between the energetic binder of C_3H_6O (trimethylene oxide) with the Al(111) surface, as the Al surface is considered to be easily exposed, easily oxidized and chemically corroded.[15-17] In this paper, we studied eight adsorption configurations of C_3H_6O on Al(111) surface to understand how the initial adsorption position of energetic binder molecule affects its adsorption reaction pathways. In addition to studying the geometries and energies of adsorptions, we investigated the density of states as well. In view of that the DFT calculations were employed to investigate the chemisorption and dissociation pathways of H_2S on the

closed packed surfaces of a number of important noble metals and transition metals,[18,19] we also studied the interaction mechanism of C_3H_6O molecules on the Al(111) surface with a periodic DFT approach.

Computational Method

The calculations performed in this study were done using the CASTEP package[20] with Vanderbilt-type ultrasoft pseudopotentials[21] and a plane-wave expansion of the wave functions. Exchange and correlation were treated with the generalized gradient approximation (GGA), using the functional form of Perdew, Burke, and Ernzerhof of PBE.[22] The electronic wave functions were obtained by a density-mixing scheme[23] and the structures were relaxed using the Broyden, Fletcher, Goldfarb, and Shannon (BFGS) method.[24] In this study, the cutoff energy of plane waves was set to 300 eV. Brillouin zone sampling was performed using the Monkhost–Pack scheme. The values of the kinetic energy cutoff and the k-point grid were determined to ensure the convergence of total energies.

A slab model with periodic boundary conditions represented the Al surface. The energy convergence with respect to the number of layers has been tested to ensure the reliability and representative of the selected model. The surface energy (E_{surf}) is calculated by equation,

$$E_{surf} = \frac{E_{slab} - nE_{bulk}}{2A} \quad (1)$$

Here E_{slab} is total energy of the selected slab supercell, E_{bulk} is the energy of the bulk crystal per atom, n is the number of atoms in the slab calculation, and A is the area of the slab. The surface energies of 1, 2 and 3 layers are 0.40 eV, 0.35 eV and 0.35 eV, respectively. Therefore, considering the balance of both computational efficiency and accuracy, a 6 × 6 supercell with three layers containing 108 Al atoms was used to study the adsorption of the molecular systems (see Figure 1). The slabs were separated by 15 Å of vacuum along the c-axis direction. The cell size with a rhombic box of a × b × c is 17.18 Å × 17.18 Å × 19.68 Å.

Several tests have been performed to verify the accuracy of the method when applied to bulk aluminum, such as the optimum cutoff energy for calculations. For bulk aluminum, we have tested for convergence, using the *k*-point sampling density and the kinetic energy cutoff. In these calculations, a Monkhorst-Pack scheme with mesh parameters of 12 × 12 × 12 has been used, leading to 56 *k*-points in the irreducible Brillouin zone. To determine the equilibrium bulk parameters of aluminum, we uniformly scaled the lattice vectors and performed energy calculations as a function of the unit-cell volume. The calculated lattice constants are the same

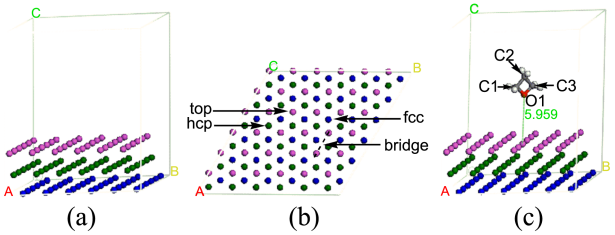

Figure 1. (a) Lateral view of the slab model of Al(111). Atoms in different layers are colored differently for easy identification. (b) Top view of the surface. Surface sites are depicted in the panel. (c) Trimethylene oxide molecule on the Al surface with no interactions.

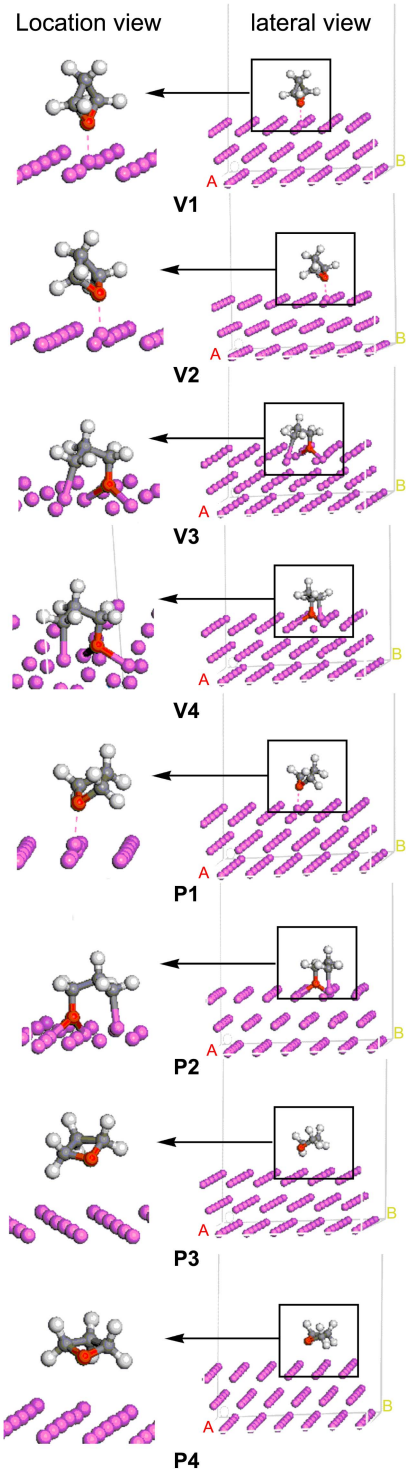

Figure 2. Adsorption configurations of trimethylene oxide on the Al(111) surface. **V** and **P** denote vertical and parallel adsorptions of trimethylene oxide, respectively.

values of 4.050 Å at E_{cut} = 300 eV and E_{cut} = 400 eV. It can be concluded that, at E_{cut} = 300 eV, the bulk structure is well converged, with respect to the cutoff energy. The calculated lattice constant of 4.050 Å is also identical to the experimental value,[25] indicating that the present set of pseudopotentials is able to provide a very good representation of the structural properties of bulk aluminum.

For the case of chemical adsorption configurations, the corresponding adsorption energy (E_{ads}) was calculated according to the expression

$$E_{ads} = E_{(adsorbate+slab)} - E_{(molecule+slab)} \quad (2)$$

where $E_{(adsorbate+slab)}$ is the total energy of the adsorbate/slab system after the C_3H_6O molecule being absorbed by Al slab and $E_{(molecule+slab)}$ is the single-point energy of the adsorbate/slab system as a whole but without interactions between EM molecule and the Al slab.

The $E_{(adsorbate+slab)}$ and $E_{(molecule+slab)}$ were calculated with the same periodic boundary conditions and the same Brillouin-zone sampling. A negative E_{ads} value corresponds to a stable adsorbate/slab system. Figure 1 shows the Al slab model, the absorbed surface sites and the configuration of C_3H_6O molecule on the Al surface atoms with no interactions of adsorbate/Al.

Transition states (TS) were located by using the complete LST/QST method.[26] Firstly, the linear synchronous transit (LST) maximization was performed, followed by an energy minimization in directions conjugated to the reaction pathway. The TS approximation obtained in that way was used to perform quadratic synchronous transit (QST) maximization. From that point, another conjugate gradient minimization was performed. The cycle was repeated until a stationary point was located. The convergence criterion of the transition state calculations was set to 0.25 eV/Å for the root-mean-square force. The activation energy is defined as: $E_a = E_{TS} - E_R$, where E_{TS} is the energy of transition state, and E_R is the sum of the energies of reactants.

Results and Discussion

There exist both physical and chemical adsorptions of C_3H_6O molecule on the Al(111) surface, and the latter case results in the ring break of the C_3H_6O molecule on the Al surface. There are three cases as Eqs. (3) to (5):

Physical adsorption, for example, see Figure 2, **P3** and **P4**. (3)

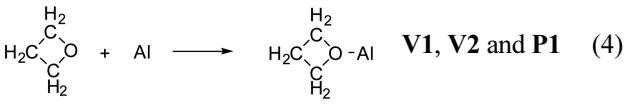

V1, **V2** and **P1** (4)

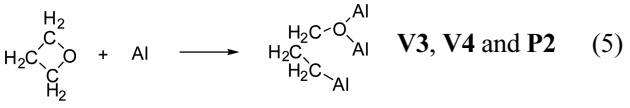

V3, **V4** and **P2** (5)

According to the orientation of the C_3H_6O ring relative to the Al(111) surface, **V** and **P** denote vertical and parallel adsorptions of C_3H_6O, respectively. The lateral views of the optimized adsorption configurations after full relaxation of the atomic positions were shown in Figure 2.

Table 1. Adsorption Energies (E_{ads}), activation energies (E_a) and Adsorption Sites of C_2H_6O on Al(111) surface

Direction of C_3H_6O on Al(111)	Conf.	Site	E_{ads} kJ/mol	E_a kJ/mol
Vertical	**V1**	top	−40.0	–
	V2	bridge	−39.9	–
	V3	hcp	−256.4	133.3
	V4	fcc	−260.1	166.8
Parallel	**P1**	top	−39.8	–
	P2	bridge	−261.9	174.0
	P3	hcp	−7.4	–
	P4	fcc	−1.8	–

Geometries and Energies. The adsorption energies were calculated by Eq. (2) and given in Table 1. As Figure 2 shows, C_3H_6O molecule is initially vertical to the Al surface and the O1 atom is above an on-top site, a bridge site, an hcp site, and an fcc site for **V1** to **V4**, respectively. **P1** to **P4** is the adsorption configuration that C_3H_6O molecule was initially parallel to the Al surface and the O1 atom is above an on-top site, a bridge site, an hcp site, and an fcc site, respectively.

Adsorption at **V1**, **V2** and **P1** sites lead to an electrostatic interaction between O atom and Al atom, as Eq. (4). These three configurations illustrates that the C_3H_6O molecule moves toward the Al surface, and the O atom interacts with an Al atom underneath with electrostatic force (the distances between O and Al atoms are in range of 1.983–2.069 Å). In configurations **V3**, **V4** and **P2**, the adsorption leads to the ring break between the O atom and C1 or C3 atom. The C and O atoms adsorb on Al surface, resulting in a total of one Al−C bond and two Al−O bonds forms as Eq. (5) shows. The Al−O and Al−C bond lengths are in the range of 1.898–1.970 Å and 2.003–2.039 Å, respectively. In **P3** and **P4** configurations, our study indicated that the C_3H_6O molecule rotates to maximize the interaction with the Al surface during the optimization. As a result, the C_3H_6O molecule is nondissociative and physical adsorbed on Al(111) surface as shown in Eq. (3).

As can be seen from Table 1, the E_{ads} values of **P3** and **P4** (−7.4 kJ/mol and −1.8 kJ/mol) are the smallest, since there is no bond formed and only intermolecular forces between C_3H_6O molecule and Al surface. The E_{ads} values of **V1**, **V2** and **P1** are similar (−40.0 kJ/mol, −39.9 kJ/mol and −39.8 kJ/mol), since there is only electrostatic interaction between O atom and Al atom underneath without ring broken in each configuration (the Mulliken charges on O and Al atoms are **V1**: O −0.500 e, Al +0.310 e; **V2**: O −0.500 e, Al +0.320 e; **P1**: O −0.500 e, Al +0.320 e). Otherwise, when the ring of C_3H_6O molecule is broken, the corresponding adsorption energies are very large. The adsorption energy of **V3**, **V4** and **P2** are −256.4, −260.1 and −261.9 kJ/mol, respectively. The corresponding adsorption energies are almost the same since the decomposition products of **V3**, **V4** and **P2** are

similar.

As a whole, when the decompositions in **V3**, **V4** and **P2** configurations led to the ring open of C_3H_6O molecule, their adsorption energies are larger than those of physical adsorptions (Coulomb force and van der Waals' force). Herein, these O and C radicals readily oxidize the Al and form strong Al−O and Al−C bonds. In a word, for all the above mentioned configurations, the C_3H_6O molecule is adsorbed or decomposed to different products when initially being placed on different surface sites, resulting in physical adsorption or strong chemical adsorptions. In addition to the formation of strong Al−O bonds, the Al−C bonds are also formed through the strong interaction of C atoms with the surface Al atoms. The fact that the dissociation of the C_3H_6O on the Al(111) surface was observed in simple energy minimizations suggests that the uncoated Al surface is very active to the electron acceptors as further discussed below.

The Density of States (DOS). The electronic structure is intimately related to their fundamental physical and chemical properties. Moreover, the electronic structures and properties are related to the adsorptions and decompositions for the adsorbates. The discussion above suggests that the decomposition of the C_3H_6O molecule on the Al surface initiates from the rupture of C−O bond and results in the formation of Al−O and Al−C bonds. Therefore, the knowledge of their electronic properties appears to be useful for further understanding the behaviors of C_3H_6O molecule on Al surface. Figure 3 displays the calculated partial DOS (PDOS) of the C, O and Al atoms from −25 to 2.5 eV for all adsorption configurations. The electronic structures vary with adsorption configurations due to the differently adsorption products of C_3H_6O on Al(111) surface.

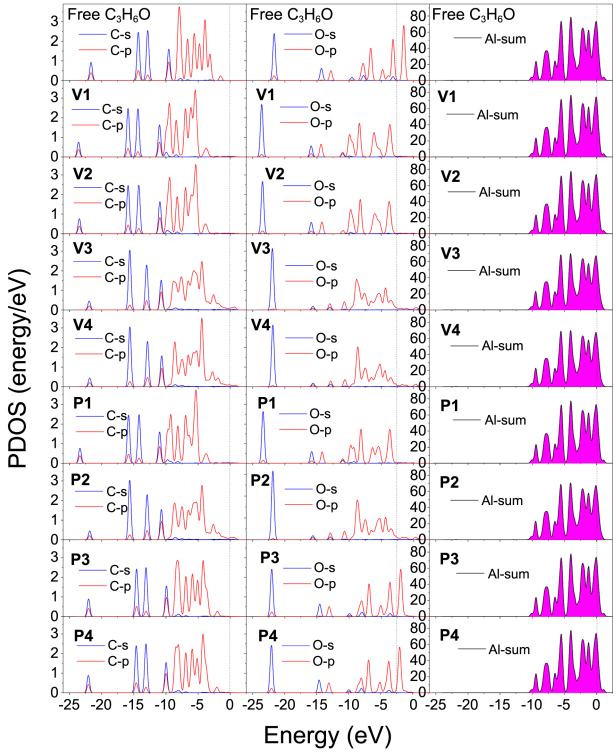

Figure 3. The PDOS for the trimethylene oxide molecule and the absorbed Al atoms, the Fermi energy is set to zero.

As can be seen from Figure 3, the PDOS peaks are similar among **V1**, **V2** and **P1** configurations and change greatly as compared to those without C_3H_6O/Al interaction. The values of the peaks become smaller and shift down −2.5 eV for both C and O atoms. Hence, the shifts of energy can be attributed to the electrostatic interaction between O atom and Al atom underneath. For **V3**, **V4** and **P2**, the adsorption reaction leads to the ring break between the O atom and C1 or C3 atom. The C and O atoms adsorb on Al surface, resulting in a total of one Al−C bond and two Al−O bonds. Since the adsorption products are almost same, the PDOS of C and O atoms are similar to each other as well. In the range of −10 to −2.5 eV, the peaks become smoother, whereas the number of DOS peaks becomes more, as compared to free C_3H_6O. For C atoms, the PDOS overlaps partly with Al DOS at Femi energy (0 eV), which is caused by the formation of Al−C bond. Similarly, the PDOS of O atom also overlaps with Al DOS at Femi energy since two Al−O bonds formed. Finally, in **P3** and **P4** configurations, for both C and O atoms, the values and shape of the peaks almost similar to those of free C_3H_6O. It is because that the C_3H_6O molecule is parallel to the Al surface and is only physically adsorbed on Al surface.

For all adsorption configurations, the DOS of Al atoms changes slightly. At the range of −12.5 to 2.5 eV, the DOS of Al atoms with C and O atoms overlap in different degrees. From the above analysis we can draw that when the bonding interactions between the absorbates and the Al surface are strengthened, the PDOS shifts and becomes smoother with respect to those of free C_3H_6O molecule. These explain the dissociation of C−O bonds and the formation of strong Al−O

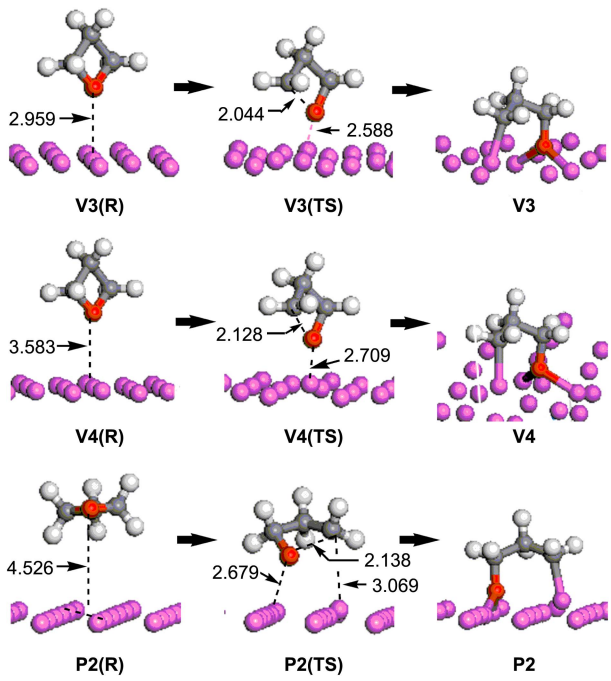

Figure 4. Lateral views of trimethylene oxide on the Al(111) surface. The index **R** and **TS** denote the reactant and transition state, respectively.

and Al−C bonds and show that the interaction between C_3H_6O and Al results in the overlaps of the electronic outer orbitals between Al and O or C atoms of C_3H_6O.

The Mechanism of Dissociation. The reactants (R), transition state (TS) and products for the surface reaction of C_3H_6O molecule on the Al(111) were depicted in Figure 4, and a detailed energy profile for three dissociation of adsorbed C_3H_6O configurations were presented in Figure 5. The activation energies and reaction energies at transition state were tabulated in Table 1.

As can been seen from Figure 4, for **V3**, **V4** and **P2**, the C_3H_6O molecule interacts with surface Al atoms and make the Al atoms underneath deviate from the first layer obviously. For **V3** configurations, the C_3H_6O molecule is initially vertical to the Al surface at the hcp site and 2.959 Å above the Al(111) surface. In **V3(TS)**, The C1-O1 bond ruptures, and the distance between C1 and O1 increases from 1.470 to 2.044 Å, while the bond length of C3-O1 bond decreases from 1.469 to 1.221 Å. After the transition state, the C1 and O1 atoms bind to the surface and form one Al−C bond and two Al−O bonds (in **V3**). The activation energy (E_a) is 133.3 kJ/mol, which is the lowest among the three decomposition paths, indicating that this process is easier to occur than the rest two paths. In **V4**, the reaction process is similar to **V3**. The C_3H_6O molecule is also initially vertical to the Al surface at fcc site and 3.583 Å above the Al(111) surface. With the reaction going on, C1−O1 bond breaks and the distances between the C1 and O1 atoms increases to 2.128 Å and the distance between O1 and the nearest Al atoms is 2.709 Å. As compared to **V3(TS)**, the activation energy (E_a) of **V4(TS)** is 166.3 kJ/mol and a little higher than **V3(TS)**, which shows that the reaction barrier for fcc adsorption site is higher than the barrier of hcp site, since the **V3(TS)** is slightly closer to Al(111) surface and the interaction between **V3(TS)** and Al facilitates the C_3H_6O dissociation. Finally, for **P2(TS)**, the C_3H_6O molecule is initially parallel to the Al surface at bridge site and 4.526 Å above the Al(111) surface, as the reaction going on, the C_3H_6O molecule moves towards the Al surface and the C3−O1 bond breaks. The distance between the C3 and O1 atoms increases to 2.138 Å and the distance between O1 atom and the nearest Al atom is 2.679 Å, as well as the distance between C3 atom and the nearest Al atom is 3.069 Å. The activation energy (E_a) of this transition is 174.0 kJ/mol (see Table 1 and Figure 5), which is the highest E_a among the three dissociation paths, and suggests that repulsive interaction between Al and H atoms promote the reaction barrier. With the decomposition process going on, the broken C_3H_6O molecule binds with the surface Al atoms and form one Al−C bond and two Al−O bonds (see **P2**).

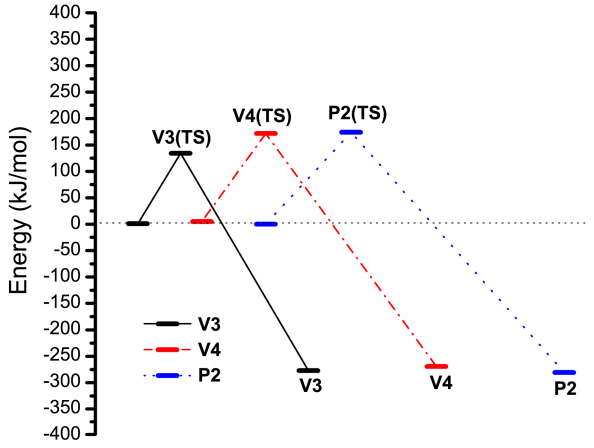

Figure 5. Relative energy profile for trimethylene oxide adsorption on the Al(111) surfaces.

Conclusions

Based on the investigation of C_3H_6O molecule on Al(111) surface, the major findings can be summarized as follows.

(1) There exist both physical and chemical adsorptions when the C_3H_6O molecule approaches the Al surface. The oxygen atom of the adsorbed C_3H_6O molecule readily oxidizes the Al surface. Dissociations of the C−O bond result in the formations of strong Al−O and Al−C bonds.

(2) The PDOS projections on the C and O atoms for the dissociated C−O bond adsorptions occur with an obvious shift of peaks, which infers that energy bands become broad and the interactions of chemical bonds are strengthened.

(3) The decomposition processes on Al surface were predicted to be exothermic. The activation energy for **V3**, **V4** and **P2** configurations are 133.3, 166.8 and 174.0 kJ/mol, respectively. The hcp site is the most reactive position for the chemical adsorption of C_3H_6O molecules.

Acknowledgments. We gratefully acknowledge the funding provided by the Laboratory of Science and Technology on Combustion and Explosion (Grant No. 9140C3501021101) for supporting this work. C.-C. Ye. thanks the Innovation Project for Postgraduates in Universities of Jiangsu Province (Grant No. CXZZ13_0213) and the Innovation Foundation from the Graduate School of NJUST for partial financial support.

References

1. Yang, V.; Brill, T. B.; Ren, W. Z. *Solid Propellant Chemistry, Combustion, and Motor Interior Ballistics*; American Institute of Aeronautics and Astronautics: Reston, Va., 2000.
2. Brenner, D. W.; Robertson, D. H.; Elert, M. L.; White, C. T. *Phys. Rev. Lett.* **1993**, *70*, 2174.
3. Yetter, R. A.; Dryer, F. L.; Allen, M. T.; Gatto, J. L. *J. Propul. Power.* **1995**, *11*, 683.
4. Bucher, P.; Yetter, R. A.; Dryer, F. L.; Vicenzi, E. P.; Parr, T. P.; Hanson-Parr, D. M. *Combust. Flame* **1999**, *117*, 351.
5. Umezawa, N.; Kalia, R. K.; Nakano, A.; Vashista, P.; Shimojo, F. *J. Chem. Phys.* **2007**, *126*, 234702.
6. Guadarrama-Perez, C.; Martinez de La Hoz, J. M.; Balbuena, P. B. *J. Phys. Chem. A* **2010**, *114*, 2284.
7. Thompson, D. L.; Sorescu, D. C.; Boatz, J. A. *J. Phys. Chem. B* **2005**, *109*, 1451.
8. Sorescu, D. C.; Boatz, J. A.; Thompson, D. L. *J. Phys. Chem. A* **2001**, *105*, 5010.
9. Sorescu, D. C.; Boatz, J. A.; Thompson, D. L. *J. Phys. Chem. B* **2003**, *107*, 8953.

10. Sutton, G. P.; Biblarz, O. *Rocket Propulsion Elements*; Wiley: Hoboken, N.J., 2010.
11. Ye, C. C.; Ju, X. H.; Zhao, F. Q.; Xu, S. Y. *Chinese J. Chem.* **2012**, *30*, 2539.
12. Zhou, S. Q.; Zhao, F. Q.; Ju, X. H.; Cheng, X. C.; Yi, J. H. *J. Phys. Chem. C* **2010**, *114*, 9390.
13. Ye, C. C.; Zhao, F. Q.; Xu, S. Y.; Ju, X. H. *J. Mol. Model* **2013**, *19*, 2451.
14. Ye, C. C.; Zhao, F. Q.; Xu, S. Y.; Ju, X. H. *Can. J. Chem.* **2013**, *91*, 1207.
15. Johnson, O. *J. Catal.* **1973**, *28*, 503.
16. Hoffmann, R. *Solids and Surfaces: A Chemist's View of Bonding in the Extended Structures*; VCH Publishers: New York, 1988.
17. Chatterjee, A.; Niwa, S.; Mizukami, F. *J. Mol. Graph.* **2005**, *23*, 447.
18. Alfonso, D. R. *Surf. Sci.* **2008**, *602*, 2758.
19. Alfonso, D. R.; Cugini, A. V.; Sorescu, D. C. *Catal. Today* **2005**, *99*, 315.
20. Segall, M. D.; Lindan, P. J. D.; Probert, M. J.; Pickard, C. J.; Hasnip, P. J.; Clark, S. J.; Payne, M. C. *J. Phys-Condens Mat.* **2002**, *14*, 2717.
21. Perdew, J. P.; Chevary, J. A.; Vosko, S. H.; Jackson, K. A.; Pederson, M. R.; Singh, D. J.; Fiolhais, C. *Phys. Rev. B, Condens. Mat.* **1992**, *46*, 6671.
22. Perdew, J. P.; Burke, K.; Ernzerhof, M. *Phys. Rev. Lett.* **1996**, *77*, 3865.
23. Kresse, G.; Furthmuller, J. *Phys. Rev. B* **1996**, *54*, 11169.
24. Fischer, T. H.; Almlof, J. *J. Phys. Chem.* **1992**, *96*, 9768.
25. King, H. W. *CRC Handbook of Chemistry and Physics*; CRC Press: Boca Raton, FL, 2000.
26. Halgren, T. A.; Lipscomb, W. N. *Chem. Phys. Lett.* **1977**, *49*, 225.